

# Electron Transport through Conjugated Molecules: When the $\pi$ System Only Tells Part of the Story

Gemma C. Solomon,\* David Q. Andrews,\* Richard P. Van Duyne, and Mark A. Ratner<sup>[a]</sup>

*In molecular transport junctions, current is monitored as a function of the applied voltage for a single molecule assembled between two leads. The transport is modulated by the electronic states of the molecule. For the prototypical delocalized systems, namely,  $\pi$ -conjugated aromatics, the  $\pi$  system usually dominates the transport. Herein, we investigate situations where model calculations including only the  $\pi$  system do not capture all of the subtleties of the transport properties. Including both the  $\sigma$  and  $\pi$  contributions to charge transport allows us to demonstrate*

*that while there is generally good agreement, there are discrepancies between the methods. We find that model calculations with only the  $\pi$  system are insufficient where the transport is dominated by quantum interference and cases where geometric changes modulate the coupling between different regions of the  $\pi$  system. We examine two specific molecular test cases to model these geometric changes: the angle dependence of coupling in (firstly) a biphenyl and (secondly) a nitro substituent of a cross-conjugated unit.*

## 1. Introduction

Many properties of conjugated molecules are dominated by the characteristics of the  $\pi$  system, and electron transfer and transport are no exception. Experimental and theoretical studies of single-molecule transport have focused considerable efforts on conjugated molecules, with the hope that versatile electronic devices can be engineered from these building blocks. The assumption that the properties of the  $\pi$  system would dominate the transport in these systems was wide-ranging. Indeed, there were many theoretical studies using Hückel models which only included the  $\pi$  system of the molecule. The success of these methods indicates that there are many situations in which the  $\sigma$  system may be neglected without consequence. However, this need not always be the case.

One area in which there has been extensive work with Hückel models,<sup>[1–20]</sup> as well as recent calculations with more realistic approaches,<sup>[15, 18, 21–23]</sup> is the prediction of systems where quantum-interference effects dominate the molecular transport. These systems constitute a particularly good test case as the transmission through a system dominated by destructive interference will be in stark contrast to one with constructive interference. Previous work comparing Hückel model calculations with more realistic approaches<sup>[15, 18]</sup> has noted that, broadly speaking, the same features are observed. However, the quantitative differences between the approaches may be extreme. In particular, the sharp interference features seen in Hückel model calculations are not observed. The interference feature in question suppresses  $\pi$ -system transport, thus leading to the question: is the  $\sigma$  system transport still insignificant in this regime?

We proceed by looking at two classes of molecules where quantum interference effects have been seen. First, in substituted phenyl rings, which constitute one of the best-studied systems in this area; and second, in acyclic cross-conjugated molecules, which have been identified more recently as exhib-

iting these characteristics. In the second part of this paper we look at two systems with geometric modifications and examine the effects on transmission and conductance as a dihedral angle is changed, either in the backbone or to a substituent. Both of these changes decouple segments of the  $\pi$  system.

## Methods

**Hückel-Model Calculations:** The Hückel-model calculations performed in this area treat only the  $\pi$  electrons in conjugated molecular systems. A simple multisite model Hamiltonian can be constructed by representing each site with the site energy  $\alpha$ . Between chemically bonded, nearest-neighbor sites there are coupling elements,  $\beta$ , and all other elements are zero.

For example, in Figure 1, two models for the two-site systems are shown. These systems differ only in their attachment to the electrodes, so the Hückel Hamiltonian for the molecular part is the same [Eq. (1)]:

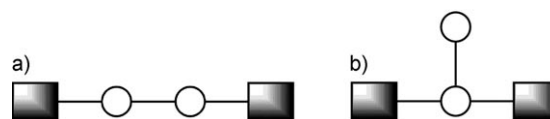


**Figure 1.** Two two-site models: a) linear model; b) branched model.

[a] Dr. G. C. Solomon, Dr. D. Q. Andrews, Prof. R. P. Van Duyne, Prof. M. A. Ratner  
Department of Chemistry, Northwestern University  
Evanston, IL, 60208 (USA)  
Fax: (+1) 847-491-7713  
E-mail: g-solomon@northwestern.edu  
dqandrews@northwestern.edu

$$H_m = \begin{pmatrix} \alpha & \beta \\ \beta & \alpha \end{pmatrix} \quad (1)$$

In all calculations shown here, we set  $\alpha = 0$  eV and  $\beta = -2.7$  eV, as has been used in previous calculations in the area.<sup>[7]</sup> We assume that only a single site couples to each electrode, with coupling strength  $\gamma = \beta/3$ . For the two systems shown in Figure 1, the coupling matrix to the left lead is identical [Eq. (2)]:

$$V_L = \begin{pmatrix} \gamma & 0 \\ 0 & 0 \end{pmatrix} \quad (2)$$

The two systems are distinguished only by different coupling to the right electrode [Eq. (3)]:

$$V_{\text{linear}}^R = \begin{pmatrix} 0 & 0 \\ 0 & \gamma \end{pmatrix} \quad (3)$$

$$V_{\text{branched}}^R = \begin{pmatrix} \gamma & 0 \\ 0 & 0 \end{pmatrix}$$

The transmission is then calculated using the non-equilibrium Green's function formalism by assuming the wide-band limit for the density of states of the electrodes and setting [Eq. (4)]:

$$\Gamma^{L(R)} = 2\pi\rho V^{L(R)} V^{L(R)\dagger} \quad (4)$$

where  $\rho$  is the density of states of the electrode, which we set to one. The self energies are given by Equation (5):

$$\Sigma^{L(R)} = \frac{i\Gamma^{L(R)}}{2} \quad (5)$$

and the retarded Green's function by Equation (6):

$$G^r(E) = (E - H_m - \Sigma_L - \Sigma_R)^{-1} \quad (6)$$

where  $E$  is the energy. The advanced Green's function,  $G^a(E)$ , is the complex conjugate of  $G^r(E)$ . The transmission is then calculated as [Eq. (7)]:

$$T(E) = \text{Tr}[\Gamma^L G^r(E) \Gamma^R G^a(E)] \quad (7)$$

**Molecular Calculations:** All molecular geometries were obtained by optimizing the isolated molecule in the gas phase using Q-Chem 3.024 with density functional theory (DFT) using the B3LYP functional<sup>[25,26]</sup> and 6-311G\*\* basis. The gas-phase molecules were chemisorbed (terminal hydrogen atoms removed) to the bridge binding site of an Au(111) surface with the Au–S bond length taken from the literature.<sup>[27]</sup> While the bridge binding site is not the global minimum on the potential energy surface for a thiol binding to gold, it is energetically close,<sup>[27]</sup> and the high symmetry of the resulting configuration allows for more detailed analysis of the transmission characteristics.

All transport calculations shown here were performed using gDFTB.<sup>[28–30]</sup> No gold atoms were included in the extended molecule so that the symmetry of the molecule could be used to separate the transmission into  $\sigma$  and  $\pi$  components.<sup>[31]</sup> The electrode comprised a  $4 \times 4$  atom unit cell with three layers in the transport direction, and periodic boundary conditions were used.

## 2. Simple Systems

### 2.1. 1,3- and 1,4-Substituted Phenyl Rings

The prototypical system studied in this area is the difference in the transmission through a phenyl ring substituted at either the *meta* (1,3) or *para* (1,4) positions. This system has been studied extensively, both with Hückel-model calculations<sup>[1–4,7,8,11–20]</sup> and DFT-based methods.<sup>[15,18,21]</sup> The general conclusion is that the low transmission through the *meta*-substituted system results from destructive interference near the Fermi energy, whereas the *para*-substituted system exhibits relatively large transmission through this region. Recent work has cautioned that Hückel-model calculations may not correspond well, even in a qualitative sense, with DFT-based ones performed for the smallest systems (1,3 and 1,4 benzenedithiol).<sup>[21]</sup>

Herein, we do not investigate the smallest system but instead consider *meta*- and *para*-substituted phenyl rings with ethynyl spacers preceding the thiol terminal groups, as shown in the inset to Figure 2. These spacers allow the component considered to interact with the electrodes only through the chosen positions. Problems can arise with, for example, *meta*-substituted benzene, which has hydrogen atoms in the 4 and 6 positions that are very close to our planar electrodes without the spacer groups. Figures 2a and 2b show the total transmission through *meta*- and *para*-substituted benzene rings calculated using the Hückel model and gDFTB, respectively.

The main difference between the methods is that the sharpness of the anti-resonance feature seen in the Hückel-model calculations is not present in the total transmission calculated using gDFTB. The origin of this discrepancy can be understood by examining the symmetry-separated components of the transmission, as shown in Figure 2c. Clearly, the anti-resonance feature does exist in the  $\pi$ -system transmission for *meta*-substituted benzene; however, it is not visible in the total transmission due to the non-negligible contributions of the  $\sigma$  system to the transport. Previously, when considering the transport through fully conjugated molecules, it was assumed that the  $\sigma$ -system transport could be neglected as the  $\pi$  system would dominate, an assumption that is unfounded when considering systems where destructive interference dominates close to the Fermi energy.

Comparing this work with previous efforts in the area,<sup>[21]</sup> an additional feature of the spacer groups is evident. At the Fermi energy, the transmission through the (1,3) substituted system is controlled by the magnitude of the  $\sigma$  transport, which decreases exponentially with increasing length. Consequently, the spacer groups mean that a much larger difference between the (1,3) and (1,4) systems is evident when the  $\sigma$  transport is reduced by increasing the length of the system.

### 2.2. Branched Structures

Cyclic conjugated molecules are not the only systems where interference features are manifest. Branched structures have also been extensively investigated with Hückel-model calculations,<sup>[5,6,9,10,15,20]</sup> and recently, we examined the transport prop-

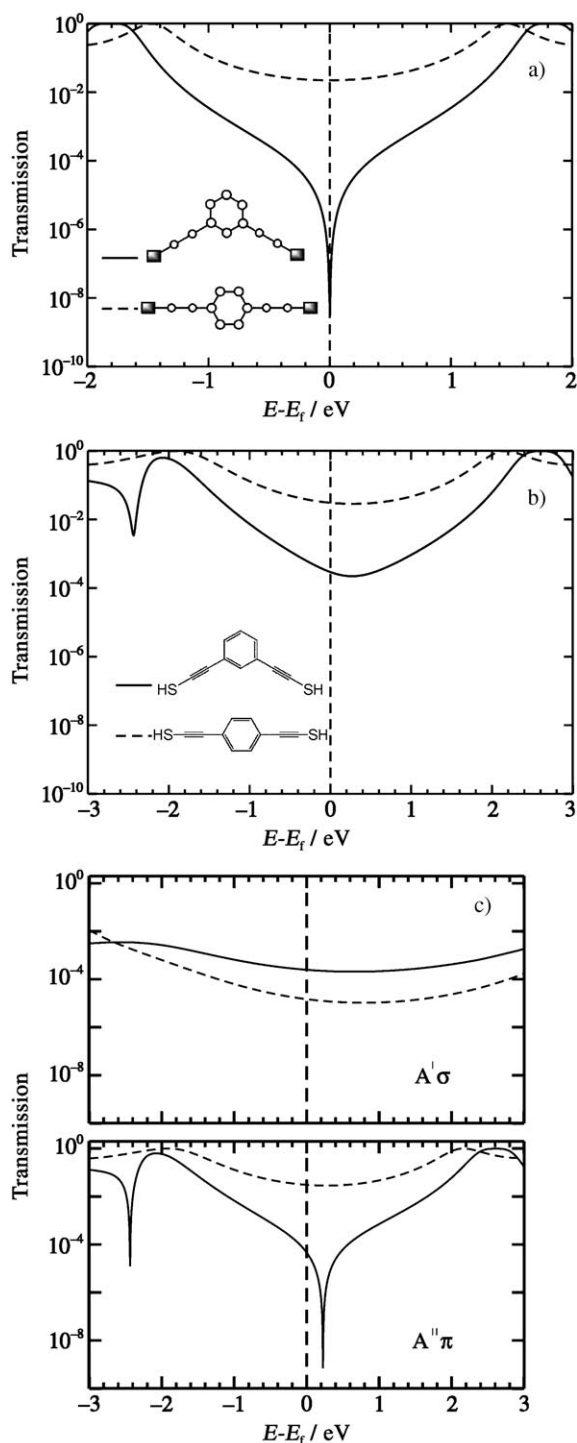


**Figure 2.** The transmission through (1,3) (—) and (1,4) (---) substituted phenyl rings as calculated by the Hückel method (a) and by gDFTB (b, c). Both the total transmission (a, b) and the symmetry-separated transmission (c) are shown.

erties of cross-conjugated molecules<sup>[22,23]</sup> as the molecular analogue. The work done with Hückel models predicted an interesting relationship between the length of the side chain and the transmission characteristics; namely, that there would be low transmission, due to an interference feature, for odd-

length side chains and high transmission for even-length side chains.<sup>[10]</sup>

In previous work with model systems, there was only minimal attention given to the backbone of the molecule; however, when molecular systems are considered, the length of the backbone is very important. The requirement that only atoms which are part of the conjugated framework are represented by sites in the Hückel model means that the length of the side chain and backbone control what type of molecule is being measured. A small change in the model can result in considerably different molecules. For example, linearly conjugated molecules must always have an even-length backbone, an even-length backbone with a single odd-length side chain must be a radical, and an odd-length backbone with a single odd-length side chain is a cross-conjugated molecule.

Figure 3 shows the transmission calculated with both the Hückel model and gDFTB for three molecules. The first represents a branched cross-conjugated molecule, the second is the comparable linearly conjugated molecule; importantly, the backbone is not of the same length in these two systems. The third molecule is the system that results when the backbone has the same length as the linearly conjugated system but a single-site side chain is added—a modification that is only possible when the molecule is a radical.

As in the phenyl systems, the  $\pi$ -system transport agrees with the Hückel-model calculations. These results also agree with the prediction that there will be an interference feature near the Fermi energy when there is an odd-length side chain.

It is interesting to note that the Hückel-model calculations reproduce well the qualitatively different transmissions through the linearly conjugated radical and the cross-conjugated molecule. The interference feature in the linearly conjugated radical system is significantly narrower than that of the cross-conjugated system, which echoes previous work where the line shape of the interference feature changed substantially in different systems.<sup>[32]</sup> The details of what controls the line shape in interference features remain as an object for future investigation. In this instance, one clear difference is that there is a molecular-orbital energy that lies directly under the interference feature in the radical system, which could well be responsible for the difference in line shape.

### 3. Geometric Modifications and Transport

In recent years, experimental methods for measuring single-molecule conductance have moved towards techniques relying on statistical distributions.<sup>[33–36]</sup> Large numbers of measurements are made, and from histograms of the data, the conductance of a single molecule can be determined. These techniques have highlighted the significant role that geometric variation, in both the molecule and the binding site on the electrode, can have on the transport. These results have been replicated using theoretical methods;<sup>[37]</sup> however, they present an interesting avenue of investigation for Hückel methods where there is no explicit geometry to change, only the changes in coupling elements and site energies that result. Herein, we will focus on one specific geometric modification:

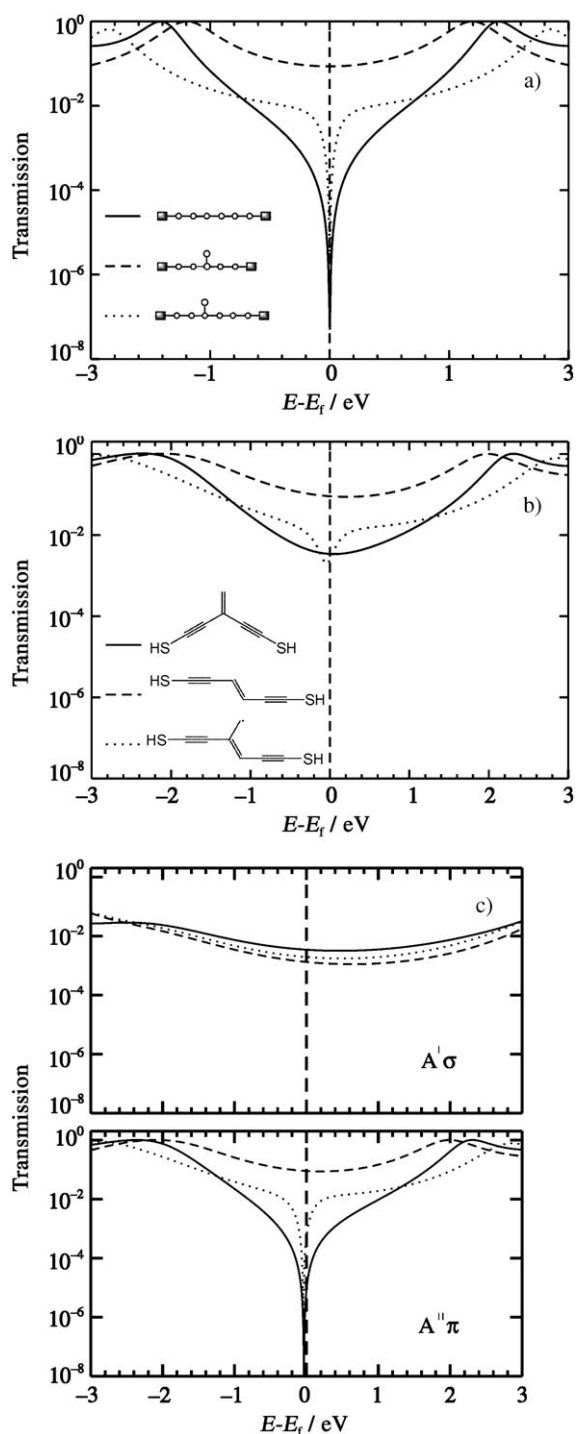


**Figure 3.** The transmission through linear (-----) and branched (— and ..... ) molecules as calculated by the Hückel method (a) and by gDFTB (b, c). Both the total transmission (a, b) and the symmetry-separated transmission (c) are shown.

changing dihedral angles to alter the coupling between parts of the  $\pi$  system.

### 3.1. Biphenyl

Quantum interference is not the only method by which transmission through a conjugated molecule may be suppressed.

Without introducing saturated groups to break conjugation, it is also possible to lower the transport through the  $\pi$  system by changing a dihedral angle and reducing the  $\pi$ -system overlap between parts of the molecule. This effect has been studied both experimentally<sup>[36]</sup> and theoretically<sup>[38]</sup> in previous work. Herein, we consider a biphenyl system and change the angle between the planes of the two phenyl rings to increase and decrease the overlap. In gDFTB, this is accomplished by taking the optimized geometry and simply changing the dihedral angle across the bond between the phenyl rings, thereby leaving all other geometrical parameters fixed. In the Hückel model, we do not have this option and instead change the coupling element between the two phenyl rings as a function of  $\theta$  [Eq. (8)]:

$$\beta_\theta = \beta \cos(\theta) \quad (8)$$

where  $\beta = -2.7$  eV, as is used for all other sites. Figures 4a and 4b illustrate the molecules considered in the two methods.

Whilst the angle  $\theta$  can be varied arbitrarily, there is a limited range with experimental significance for these unsubstituted biphenyl systems. Figure 4c shows the energy of the isolated molecule above the energy of the optimized structure for a variety of angles. The energy was calculated using a single-point calculation with the same level of theory as that used for the optimizations. The solid vertical line shows the value of  $\theta$  for the optimized geometry ( $39.96^\circ$ ). The dashed horizontal line shows the energy available to the system at room temperature and the shaded region maps the range of angles accessible as a consequence.

The transmission can be calculated using both methods for the angles ( $\theta$ ) considered above, and is shown in Figure 5. Broadly, the two methods give very similar results. There is some difference in the pattern of resonances in the transmission predicted by the two methods, but the trends are common amongst them. It is interesting to note that when transmission is suppressed by lowering the overlap between regions of the  $\pi$  system, both resonant and off-resonant transport are disrupted across the entire range, as distinct from suppression by quantum interference, where only off-resonant transport in a small energy range is disrupted as the interference feature occurs mid-way between the resonances.

The relevant range of the transport, as well as some subtle qualitative differences between the methods, can be seen by examining the zero-bias conductance as a function of the angle. The zero-bias conductance is directly related to the transmission at the Fermi energy, and consequently, the same behavior as a function of the angle is observed. Figure 6 shows the zero-bias conductance as a function of  $\theta$ , with the conductance being evaluated in two ways for each method: First, the angular dependence can be estimated by taking the conductance at  $\theta=0$  ( $G(0)$ ) and multiplying it by  $\cos^2(\theta)$ . The second way is by explicitly calculating the conductance at each angle.

The first point to note from these results is that throughout the range of angles predicted at room temperature, the conductance only varies by approximately a factor of two. Whilst

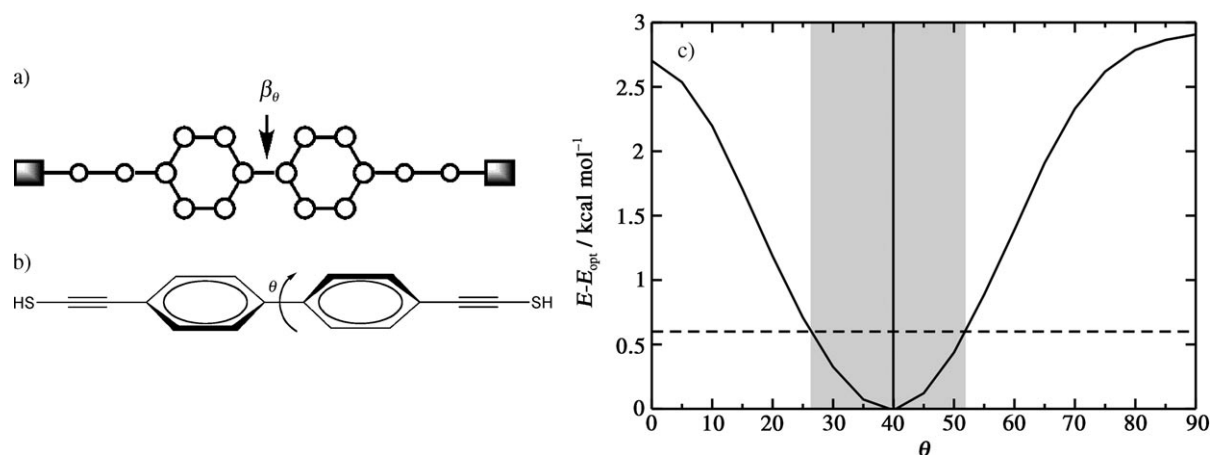


**Figure 4.** The biphenyl systems considered: a) Hückel-model system and b) gDFTB system; and the potential energy surface (c) that describes the energy of the structure above the optimized structure as a function of  $\theta$ .

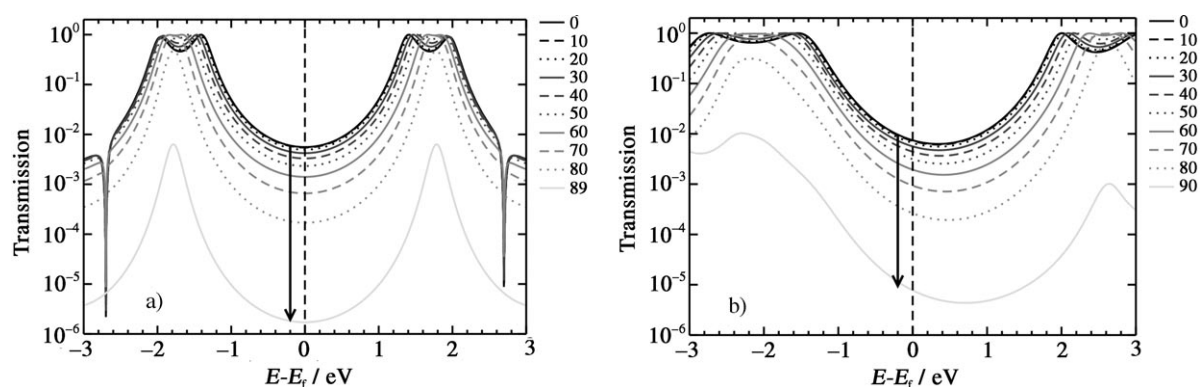


**Figure 5.** The transmission through the biphenyl system as  $\theta$  is varied from  $0^\circ$  to  $90^\circ$ , showing the suppression of the transport as the overlap between the  $\pi$  systems on the phenyl rings is reduced. a) Hückel-model transmission; b) gDFTB transmission.

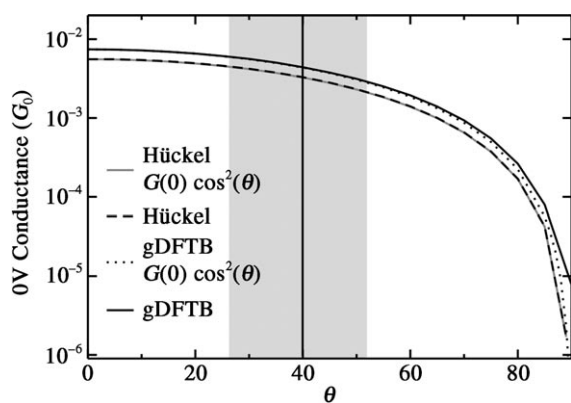


**Figure 6.** The zero-bias conductance as a function of the angle, calculated by using the Hückel method (----) and by gDFTB (—). The angular dependence is also approximated for the two methods (— and ····), showing good agreement up to high angles where the  $\sigma$  system dominates the gDFTB transport.

this might seem to be a large variation, given the four orders of magnitude change in conductance as  $\theta$  goes from  $0^\circ$  to  $90^\circ$ , it is remarkably small. The constraints of the potential

energy surface, particularly the energy barrier to increasing  $\theta$ , control the range of conductance to a very large extent.

The second point to note concerns the departure, or lack thereof, between the approximated and calculated angular dependence of the two methods. For the Hückel method, there is exact agreement between the approximated angular dependence and the calculated dependence throughout the range. This is an unsurprising result, which simply illustrates the expected behavior of a molecule in which the conductance is dominated by the  $\pi$  system. The interesting, although subtle, point is the disparity between the approximated and calculated angular dependence using gDFTB as  $\theta$  approaches  $90^\circ$ . In particular, very close to  $90^\circ$ , the calculated conductance using gDFTB is finite whereas all of the other curves go to zero. This finite conductance is, of course, the  $\sigma$ -system transport, which remains when the  $\pi$ -system transport is suppressed. Both the angular dependence and the  $\sigma$  coupling when  $\theta=90^\circ$  have been predicted previously in calculations of through molecule coupling in 4,4'-bipyridine.<sup>[38]</sup> here, we simply see the effects on molecular conductance. This behavior is well outside of the anticipated range of motion of the molecule at room temperature. Nonetheless, it is an interesting

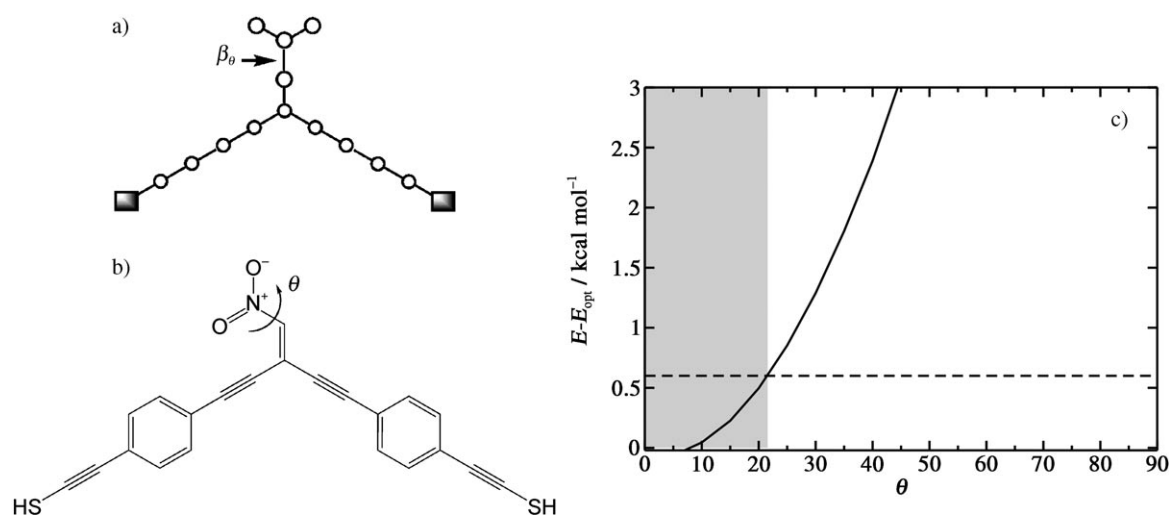


**Figure 7.** The nitro systems considered: a) Hückel-model system and b) gDFTB system; and the potential energy surface (c) that describes the energy of the structure above the optimized structure as a function of  $\theta$ .

result, which needs to be considered in any study of substituted variants where  $\theta$  may approach  $90^\circ$ .<sup>[36]</sup>

### 3.2. Substituents and Interference

Modifying a dihedral angle in a conjugated molecule need not only have the effect described in the previous part. There are components in conjugated molecules that control the main conduction path and, additionally, there may be components which tune the properties of that path. Previously, we looked at how electron-donating and electron-withdrawing substituents can tune the position of the interference feature in cross-conjugated systems.<sup>[32]</sup> In that work, we found that electron-withdrawing groups shift the position of the interference feature in the transmission spectrum to lower energy whereas electron-donating groups shift it to higher energy.

Unsurprisingly, given their strongly electron-withdrawing character, nitro groups were an effective means of shifting the position of the interference feature by 0.5–1 eV, depending on the theoretical method used. Herein, we take the nitro substituted cross-conjugated molecule considered in that study and examine the effect of the C–C–N–O dihedral angle which controls the plane of the nitro group with respect to the plane of the conjugated backbone of the molecule. Figures 7a and 7b show the two systems used in the Hückel and gDFTB calculations, respectively, to examine this effect. The length of the molecule used in gDFTB is extended so that the  $\sigma$ -system transport is suppressed and the position of the interference feature can be seen in the total transmission. As the rotation of the nitro group breaks the molecular plane of symmetry, it is not possible to perform the symmetry analysis on this system. The extension is not required for the Hückel system as there is no  $\sigma$  system. For the Hückel calculations,  $\beta = -2.7$  eV (as in the previous sections),  $\alpha = -0.8$  eV for nitrogen, and  $\alpha = -1.6$  eV for oxygen.

The potential energy surface for the rotation of the nitro group is calculated by using the same method as that applied

for the biphenyl system and is also shown in Figure 7. The optimized geometry for the molecule has  $\theta = 0$ ; thus, in this case, there is no vertical line to denote the minimum energy value. It is interesting to note that the angular range accessible at room temperature is considerably larger than that found in the biphenyl case, whilst at the same time the barrier to rotation to large  $\theta$  is considerably higher in this instance.

As for the biphenyl system, the transmission is calculated for the range of  $\theta$  values and is shown in Figure 8. In these plots, however, there is an additional curve (thick magenta), which is the transmission calculated for the two systems with the nitro group substituted for a terminal hydrogen. The transmission through this unsubstituted cross-conjugated molecule is important to distinguish the qualitative difference in the results from these two methods.

Considering first the behavior of the Hückel calculations: As  $\theta$  increases, the coupling between the site representing the nitrogen and the site representing the terminal carbon decreases in precisely the same manner as the phenyl–phenyl coupling in the biphenyl system. This results in a reduction of the electron-withdrawing influence of the nitro group, and consequently, the position of the interference feature shifts back until it reaches the position it occurs at for the unsubstituted system. Conversely, the gDFTB calculation shows a different behavior. At small values of  $\theta$ , the position of the interference feature is as expected, at lower energy but moving progressively closer to the position in the unsubstituted molecule. Above  $60^\circ$ , however, the position of the anti-resonance shifts higher than its position in the unsubstituted molecule, and the nitro group is effectively functioning as an electron-donating group.

The qualitative differences in the behavior of the two methods can be seen clearly in the plot of the zero-bias conductance as a function of the angle, shown in Figure 9. The minimum at  $60^\circ$  in the gDFTB conductance marks the transition from the nitro group acting as an electron-withdrawing group to it acting as an electron-donating group. The Hückel conductance decreases smoothly to a minimum at  $90^\circ$ .

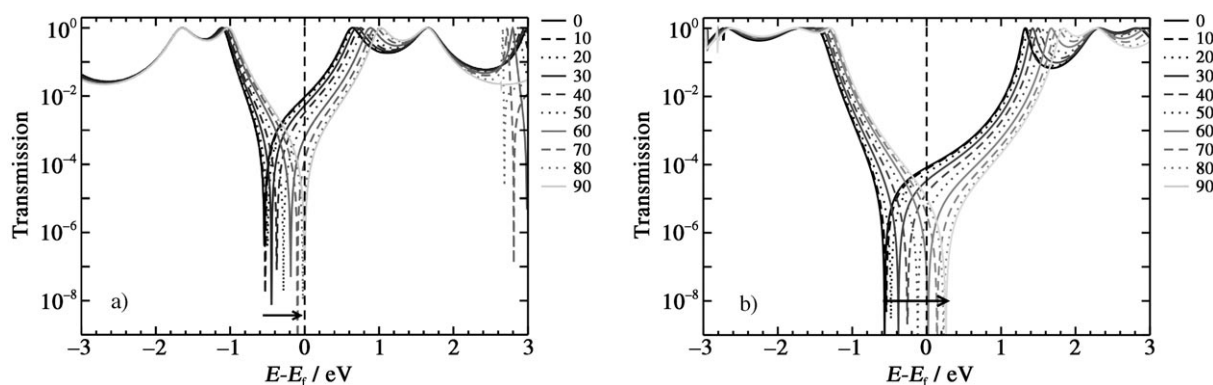


**Figure 8.** The transmission through the nitro systems as  $\theta$  is varied from  $0^\circ$  to  $90^\circ$ , showing the diminishing electron-withdrawing character of the nitro group as it is rotated out of the plane of the molecule. a) Hückel-model transmission; b) gDFTB transmission.

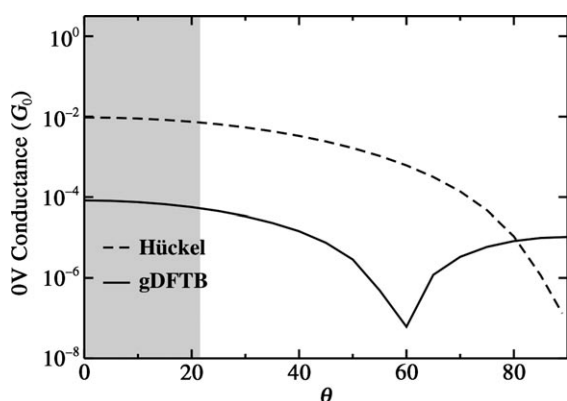


**Figure 9.** The zero-bias conductance as a function of the angle for the nitro systems calculated by using the Hückel method (----) and by gDFTB (—). The minimum in the gDFTB conductance marks the transition from the nitro group acting as electron-withdrawing to electron-donating.

At this juncture, it is important to note that this is occurring outside the range accessible at room temperature; however, it again illustrates the interesting relationship between the  $\sigma$  and  $\pi$  systems of a molecule. The electron-donating or -withdrawing effects of a substituent can act on either the  $\pi$  or the  $\sigma$  system, and as  $\theta$  changes from  $0^\circ$  to  $90^\circ$ , the  $\pi$  system of the nitro group interacts with the  $\pi$  or  $\sigma$  systems of the molecule, respectively. The electron-donating or -withdrawing character of a substituent is not an immutable parameter, but rather is dependent on the geometry, in much the same way as electron transport is itself.

#### 4. Conclusions

For all the systems considered herein, the Hückel-model calculations performed well and broadly reproduced the results obtained for the  $\pi$ -system transport through molecules calculated using gDFTB. This is a qualified success for the method, as the systems considered here also clearly showed that the  $\sigma$  system can have an important influence on the transport characteristics of fully conjugated molecules. This is of particular importance in small molecules (where the  $\sigma$  transport is

substantial) with groups that give rise to interference features, thereby suppressing the transport through the  $\pi$  system.

Furthermore, this success is only achieved when care is taken to choose chemically sensible Hückel-model systems. When simply constructing a Hückel-model Hamiltonian, it would seem that any length of molecular backbone or side chain is possible; however, this can change the nature of the conjugation or make the molecule a radical, which results in substantial changes in the transmission.

The influence of the  $\sigma$  system on the transport characteristics of a fully conjugated molecule will not normally be substantial. The systems investigated herein were only sensitive to the  $\sigma$ -system transport either when interference features dominated near the Fermi energy or when higher energy structures were considered; in this instance, the structures were outside the range accessible at room temperature. Neither of these two possibilities is likely in the majority of conjugated molecules. However, there are instances where interference features will be dominant, and the geometric effects considered may result from lower energy configurations in other molecular systems. In the case of the biphenyl system, simple synthetic modifications can lead to molecules where the local minimum on the potential energy surface occurs at values of  $\theta$  approaching  $90^\circ$ .<sup>[36]</sup> The role of electron-donating and -withdrawing groups in transport will be dependent on their ability to influence the dominant transport systems, which in turn will depend on the geometry of the molecule in question. It is possible to envisage molecules in which steric hindrance results in conformations with local minima across the range investigated for the nitro system, thereby influencing the role that such a substituent will play. In all cases, it is useful to be aware that the fact that a molecule is fully conjugated does not mean that it can be assumed that the  $\sigma$  system will play an inconsequential part in the transport.

#### Acknowledgements

We gratefully acknowledge funding from NSF-Chemistry (CHE-0719420, CHE-0414554), NSF-MRSEC (DMR-0520513), ONR-Chemistry, and the American Australian Foundation.

**Keywords:** conjugation · density functional calculations · electron transport · Hückel model ·  $\pi$  systems

- [1] P. Sautet, C. Joachim, *Chem. Phys. Lett.* **1988**, *153*, 511.
- [2] P. Sautet, C. Joachim, *Chem. Phys.* **1989**, *135*, 99.
- [3] C. Patoux, C. Coudret, J. P. Launay, C. Joachim, A. Gourdon, *Inorg. Chem.* **1997**, *36*, 5037.
- [4] C. Joachim, J. K. Gimzewski, H. Tang, *Phys. Rev. B* **1998**, *58*, 16407.
- [5] E. G. Emberly, G. Kirczenow, *J. Phys. Condens. Matter* **1999**, *11*, 6911.
- [6] T. S. Elicker, J. S. Binette, D. G. Evans, *J. Phys. Chem. B* **2001**, *105*, 370.
- [7] R. Baer, D. Neuhauser, *J. Am. Chem. Soc.* **2002**, *124*, 4200.
- [8] S. N. Yaliraki, M. A. Ratner, *Ann. N. Y. Acad. Sci.* **2002**, *960*, 153.
- [9] C. Kalyanaraman, D. G. Evans, *Nano Lett.* **2002**, *2*, 437.
- [10] R. Collepardo-Guevara, D. Walter, D. Neuhauser, R. Baer, *Chem. Phys. Lett.* **2004**, *393*, 367.
- [11] M. H. van der Veen, M. T. Rispens, H. T. Jonkman, J. C. Hummelen, *Adv. Funct. Mater.* **2004**, *14*, 215.
- [12] K. Walczak, *Cent. Eur. J. Chem.* **2004**, *2*, 524.
- [13] D. Walter, D. Neuhauser, R. Baer, *Chem. Phys.* **2004**, *299*, 139.
- [14] F. Zhai, H. Q. Xu, *Phys. Rev. B* **2005**, *72*, 195346.
- [15] M. Ernzerhof, M. Zhuang, P. Rocheleau, *J. Chem. Phys.* **2005**, *123*, 134704.
- [16] D. M. Cardamone, C. A. Stafford, S. Mazumdar, *Nano Lett.* **2006**, *6*, 2422.
- [17] M. Ernzerhof, H. Bahmann, F. Goyer, M. Zhuang, P. Rocheleau, *J. Chem. Theory Comput.* **2006**, *2*, 1291.
- [18] F. Goyer, M. Ernzerhof, M. Zhuang, *J. Chem. Phys.* **2007**, *126*, 144104.
- [19] S. K. Maiti, *Phys. Lett. A* **2007**, *366*, 114.
- [20] G. C. Solomon, D. Q. Andrews, T. Hansen, R. H. Goldsmith, M. R. Wasielewski, R. P. Van Duyne, M. A. Ratner, *J. Chem. Phys.* **2008**, *129*, 054701.
- [21] S.-H. Ke, W. Yang, H. U. Baranger, *Nano Lett.* **2008**, *8*, 3257.
- [22] G. C. Solomon, D. Q. Andrews, R. P. Van Duyne, M. A. Ratner, *J. Am. Chem. Soc.* **2008**, *130*, 7788.
- [23] D. Q. Andrews, G. C. Solomon, R. H. Goldsmith, T. Hansen, M. R. Wasielewski, R. P. V. Duyne, M. A. Ratner, *J. Phys. Chem. C* **2008**, *112*, 16991.
- [24] Y. Shao, L. F. Molnar, Y. Jung, J. Kussmann, C. Ochsenfeld, S. T. Brown, A. T. B. Gilbert, L. V. Slipchenko, S. V. Levchenko, D. P. O'Neill, R. A. DiStasio Jr., R. C. Lochan, T. Wang, G. J. O. Beran, N. A. Besley, J. M. Herbert, C. Y. Lin, T. V. Voorhis, S. H. Chien, A. Sodt, R. P. Steele, V. A. Rassolov, P. E. Maslen, P. P. Korambath, R. D. Adamson, B. Austin, J. Baker, E. F. C. Byrd, H. Dachsel, R. J. Doerksen, A. Dreuw, B. D. Dunietz, A. D. Dutoi, T. R. Furlani, S. R. Gwaltney, A. Heyden, S. Hirata, C.-P. Hsu, G. Kedziora, R. Z. Khalliulin, P. Klunzinger, A. M. Lee, M. S. Lee, W. Liang, I. Lotan, N. Nair, B. Peters, E. I. Proynov, P. A. Pieniazek, Y. M. Rhee, J. Ritchie, E. Rosta, C. D. Sherrill, A. C. Simmonett, J. E. Subotnik, H. L. W. Iii, W. Zhang, A. T. Bell, A. K. Chakraborty, *Phys. Chem. Chem. Phys.* **2006**, *8*, 3172.
- [25] A. D. Becke, *J. Chem. Phys.* **1993**, *98*, 5648.
- [26] C. Lee, W. Yang, R. G. Parr, *Phys. Rev. B* **1988**, *37*, 785.
- [27] A. Bilić, J. R. Reimers, N. S. Hush, *J. Chem. Phys.* **2005**, *122*, 094708.
- [28] D. Porezag, T. Frauenheim, T. Kohler, G. Seifert, R. Kaschner, *Phys. Rev. B* **1995**, *51*, 12947.
- [29] M. Elstner, D. Porezag, G. Jugnickel, J. Elsner, M. Haugk, T. Frauenheim, S. Suhai, G. Seifert, *Phys. Rev. B* **1998**, *58*, 7260.
- [30] A. Pecchia, A. Di Carlo, *Rep. Prog. Phys.* **2004**, *67*, 1497.
- [31] G. C. Solomon, A. Gagliardi, A. Pecchia, T. Frauenheim, A. Di Carlo, J. R. Reimers, N. S. Hush, *J. Chem. Phys.* **2006**, *125*, 184702.
- [32] D. Q. Andrews, G. C. Solomon, R. P. Van Duyne, M. A. Ratner, *J. Am. Chem. Soc.* **2008**, DOI:10.1021/ja804399q.
- [33] R. H. M. Smit, Y. Noat, C. Untiedt, N. D. Lang, M. C. van Hemert, J. M. van Ruitenbeek, *Nature* **2002**, *419*, 906.
- [34] J. Reichert, R. Ochs, D. Beckmann, H. B. Weber, M. Mayor, H. v. Löhneysen, *Phys. Rev. Lett.* **2002**, *88*, 176804.
- [35] B. Xu, N. J. Tao, *Science* **2003**, *301*, 1221.
- [36] L. Venkataraman, J. E. Klare, C. Nuckolls, M. S. Hybertsen, M. L. Steigerwald, *Nature* **2006**, *442*, 904.
- [37] D. Q. Andrews, R. P. Van Duyne, M. A. Ratner, *Nano Lett.* **2008**, *8*, 1120.
- [38] S. Woitellier, J. P. Launay, C. Joachim, *Chem. Phys.* **1989**, *131*, 481.

Received: September 7, 2008

Published online on December 29, 2008